

# Black Holes in Elliptical and Spiral Galaxies and in Globular Clusters

Reginald T. Cahill

*School of Chemistry, Physics and Earth Sciences, Flinders University,*

*Adelaide 5001, Australia*

E-mail: Reg.Cahill@flinders.edu.au

Supermassive black holes have been discovered at the centers of galaxies, and also in globular clusters. The data shows correlations between the black hole mass and the elliptical galaxy mass or globular cluster mass. It is shown that this correlation is accurately predicted by a theory of gravity which includes the new dynamics of self-interacting space. In spiral galaxies this dynamics is shown to explain the so-called ‘dark matter’ rotation-curve anomaly, and also explains the earth based bore-hole  $g$  anomaly data. Together these effects imply that the strength of the self-interaction dynamics is determined by the fine structure constant. This has major implications for fundamental physics and cosmology.

## 1 Introduction

Our understanding of gravity is based on Newton’s modelling of Kepler’s phenomenological laws for the motion of the planets within the solar system. In this model Newton took the gravitational acceleration field to be the fundamental dynamical degree of freedom, and which is determined by the matter distribution; essentially via the ‘universal inverse square law’. However the observed linear correlation between masses of black holes with the masses of the ‘host’ elliptical galaxies or globular clusters suggests that either the formation of these systems involves common evolutionary dynamical processes or that perhaps some new aspect to gravity is being revealed. Here it is shown that if rather than an acceleration field a velocity field is assumed to be fundamental to gravity, then we immediately find that these black hole effects arise as a space self-interaction dynamical effect, and that the observed correlation is simply that  $M_{BH}/M = \alpha/2$  for spherical systems, where  $\alpha$  is the fine structure constant ( $\alpha = e^2/\hbar c = 1/137.036$ ), as shown in Fig.1. This dynamics also manifests within the earth, as revealed by the bore hole  $g$  anomaly data, as in Fig.2. It also offers an explanation of the ‘dark matter’ rotation-velocity effect, as illustrated in Fig.3. This common explanation for a range of seemingly unrelated effects has deep implications for fundamental physics and cosmology.

## 2 Modelling Gravity

Let us phenomenologically investigate the consequences of using a velocity field  $\mathbf{v}(\mathbf{r}, t)$  to be the fundamental dynamical degree of freedom to model gravity. The gravitational acceleration field is then defined by the Euler form

$$\begin{aligned} \mathbf{g}(\mathbf{r}, t) &\equiv \lim_{\Delta t \rightarrow 0} \frac{\mathbf{v}(\mathbf{r} + \mathbf{v}(\mathbf{r}, t)\Delta t, t + \Delta t) - \mathbf{v}(\mathbf{r}, t)}{\Delta t} \\ &= \frac{\partial \mathbf{v}}{\partial t} + (\mathbf{v} \cdot \nabla) \mathbf{v} \end{aligned} \quad (1)$$

This form is mandated by Galilean covariance under change of observer. A minimalist non-relativistic modelling of the dynamics for this velocity field gives a direct account of the various phenomena noted above; basically the Newtonian formulation of gravity missed a key dynamical effect that did not manifest within the solar system.

In terms of the velocity field Newtonian gravity dynamics involves using  $\nabla \cdot$  to construct a rank-0 tensor that can be related to the matter density  $\rho$ . The coefficient turns out to be the Newtonian gravitational constant  $G$ .

$$\nabla \cdot \left( \frac{\partial \mathbf{v}}{\partial t} + (\mathbf{v} \cdot \nabla) \mathbf{v} \right) = -4\pi G \rho, \quad (2)$$

This is clearly equivalent to the differential form of Newtonian gravity,  $\nabla \cdot \mathbf{g} = -4\pi G \rho$ . Outside of a spherical mass  $M$  (2) has solution (we assume  $\nabla \times \mathbf{v} = \mathbf{0}$ , then  $(\mathbf{v} \cdot \nabla) \mathbf{v} = \frac{1}{2} \nabla(\mathbf{v}^2)$ )

$$\mathbf{v}(\mathbf{r}) = -\sqrt{\frac{2GM}{r}} \hat{\mathbf{r}}, \quad (3)$$

for which (1) gives the usual inverse square law

$$\mathbf{g}(\mathbf{r}) = -\frac{GM}{r^2} \hat{\mathbf{r}}. \quad (4)$$

The simplest non-Newtonian dynamics involves the two rank-0 tensors constructed at 2nd order from  $\partial v_i / \partial x_j$

$$\nabla \cdot \left( \frac{\partial \mathbf{v}}{\partial t} + (\mathbf{v} \cdot \nabla) \mathbf{v} \right) + \frac{\alpha}{8} (tr D)^2 + \frac{\beta}{8} tr(D^2) = -4\pi G \rho, \quad (5)$$

$$D_{ij} = \frac{1}{2} \left( \frac{\partial v_i}{\partial x_j} + \frac{\partial v_j}{\partial x_i} \right), \quad (6)$$

and involves two arbitrary dimensionless constants. The velocity in (3) is also a solution to (5) if  $\beta = -\alpha$ , and we then define

$$C(\mathbf{v}, t) = \frac{\alpha}{8} ((tr D)^2 - tr(D^2)). \quad (7)$$

Hence the modelling of gravity by (5) and (1) now involves two gravitational constants  $G$  and  $\alpha$ , with  $\alpha$  being the strength of the self-interaction dynamics, but which was not apparent in the solar system dynamics. We now show that all the various phenomena discussed herein imply that  $\alpha$  is the fine structure constant  $\approx 1/137$  up to experimental errors [1]. Hence non-relativistic gravity is a more complex phenomenon than currently understood. The new key feature is that (5) has a one-parameter  $\mu$  class of vacuum ( $\rho = 0$ ) ‘black hole’ solutions in which the velocity field self-consistently maintains the singular form

$$\mathbf{v}(\mathbf{r}) = -\mu r^{-\alpha/4} \hat{\mathbf{r}}. \quad (8)$$

This class of solutions will be seen to account for the ‘black holes’ observed in galaxies and globular cluster. As well this velocity field, from (1), gives rise to a non- ‘inverse square law’ acceleration

$$\mathbf{g}(\mathbf{r}) = -\frac{\alpha \mu}{4} r^{-(1+\alpha/4)} \hat{\mathbf{r}}. \quad (9)$$

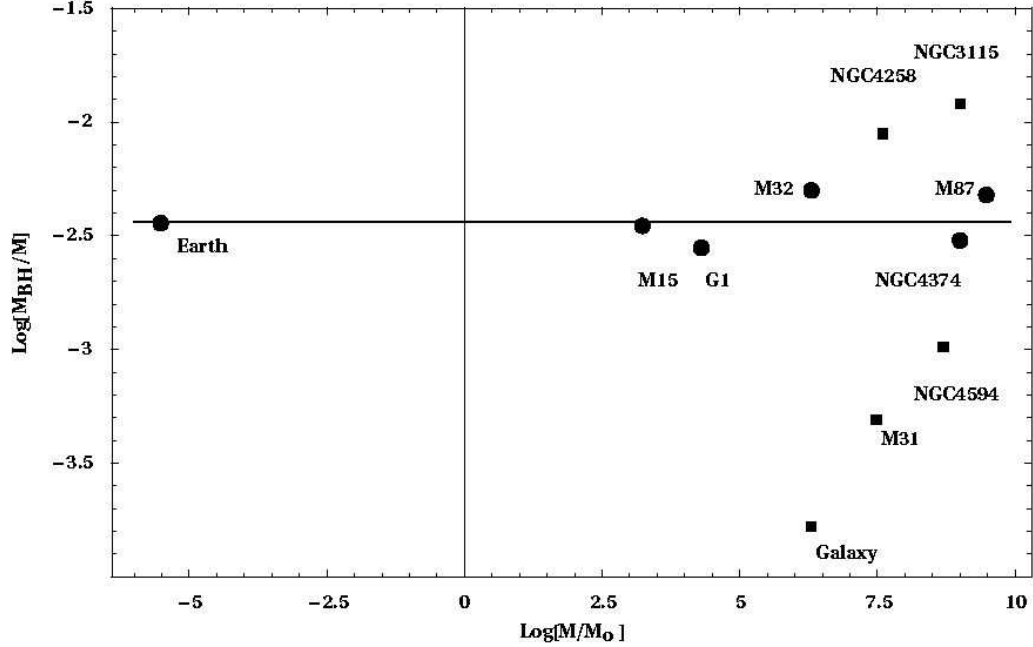


Figure 1: The data shows  $\text{Log}_{10}[M_{BH}/M]$  for the ‘black hole’ or ‘dark matter’ masses  $M_{BH}$  for a variety of spherical matter systems with masses  $M$ , shown by solid circles, plotted against  $\text{Log}_{10}[M/M_0]$ , where  $M_0$  is the solar mass, showing agreement with the ‘ $\alpha/2$ -line’ ( $\text{Log}_{10}[\alpha/2] = -2.44$ ) predicted by (17), and ranging over 15 orders of magnitude. The ‘black hole’ effect is the same phenomenon as the ‘dark matter’ effect. The data ranges from the earth, as observed by the bore hole  $g$  anomaly, to globular cluster M15 [5, 6] and G1 [7], and then to spherical ‘elliptical’ galaxies M32 (E2), NGC 4374 (E1) and M87 (E0). Best fit to the data from these star systems gives  $\alpha = 1/134$ , while for the earth data in Fig.2  $\alpha = 1/139$ . A best fit to all the spherical systems in the plot gives  $\alpha = 1/136$ . In these systems the ‘dark matter’ or ‘black hole’ spatial self-interaction effect is induced by the matter. For the spiral galaxies, shown by the filled boxes, where here  $M$  is the bulge mass, the black hole masses do not correlate with the ‘ $\alpha/2$ -line’. This is because these systems form by matter in-falling to a primordial black hole, and so these systems are more contingent. For spiral galaxies this dynamical effect manifests most clearly via the non-Keplerian rotation-velocity curve, which decrease asymptotically very slowly, as shown in Fig.3, as determined by the small value of  $\alpha \approx 1/137$ . The galaxy data is from Table 1 of [8, updated].

This turns out to be the cause of the so-called ‘dark-matter’ effect observed in spiral galaxies. For this reason we define

$$\rho_{DM}(\mathbf{r}) = \frac{\alpha}{32\pi G}((tr D)^2 - tr(D^2)), \quad (10)$$

so that (5) and (1) can be written as

$$\nabla \cdot \mathbf{g} = -4\pi G\rho - 4\pi G\rho_{DM}, \quad (11)$$

which shows that we can think of the new self-interaction dynamics as generating an effective ‘dark matter’ density.

### 3 Spherical Systems

It is sufficient here to consider time-independent and spherically symmetric solutions of (5) for which  $v$  is radial. Then we have the integro-differential form for (5)

$$v^2(r) = 2G \int d^3s \frac{\rho(s) + \rho_{DM}(v(s))}{|\mathbf{r} - \mathbf{s}|}, \quad (12)$$

$$\rho_{DM}(v(r)) = \frac{\alpha}{8\pi G} \left( \frac{v^2}{2r^2} + \frac{vv'}{r} \right). \quad (13)$$

as  $\nabla^2 \frac{1}{|\mathbf{r}-\mathbf{s}|} = -4\pi\delta^4(\mathbf{r}-\mathbf{s})$ . This then gives

$$v^2(r) = \frac{8\pi G}{r} \int_0^r s^2 ds [\rho(s) + \rho_{DM}(v(s))] + 8\pi G \int_r^\infty s ds [\rho(s) + \rho_{DM}(v(s))] \quad (14)$$

on doing the angle integrations. We can also write (5) as a non-linear differential equation

$$2\frac{vv'}{r} + (v')^2 + vv'' = -4\pi G\rho(r) - 4\pi G\rho_{DM}(v(r)). \quad (15)$$

### 4 Minimal Black Hole Systems

There are two classes of solutions when matter is present. The simplest is when the black hole forms as a consequence of the velocity field generated by the matter, this generates what can be termed an induced minimal black hole. This is in the main applicable to systems such as planets, stars, globular clusters and elliptical galaxies. The second class of solutions correspond to non-minimal black hole systems; these arise when the matter congregates around a pre-existing ‘vacuum’ black hole. The minimal black holes are simpler to deal with, particularly when the matter system is spherically symmetric. In this case the non-Newtonian gravitational effects are confined to within the system. A simple way to arrive at this property is to solve (14) perturbatively. When the matter density is confined to a sphere of radius  $R$  we find on iterating (14) that the ‘dark matter’ density is confined to that sphere, and that consequently  $g(r)$  has an inverse square law behaviour outside of the sphere. Iterating (14) once we find inside radius  $R$  that

$$\rho_{DM}(r) = \frac{\alpha}{2r^2} \int_r^R s\rho(s)ds + O(\alpha^2). \quad (16)$$

and that the total ‘dark matter’

$$\begin{aligned} M_{DM} &\equiv 4\pi \int_0^R r^2 dr \rho_{DM}(r) \\ &= \frac{4\pi\alpha}{2} \int_0^R r^2 dr \rho(r) + O(\alpha^2) \\ &= \frac{\alpha}{2} M + O(\alpha^2), \end{aligned} \quad (17)$$

where  $M$  is the total amount of (actual) matter. Hence to  $O(\alpha)$   $M_{DM}/M = \alpha/2$  independently of the matter density profile. This turns out to be a very useful property as

knowledge of the density profile is then not required in order to analyse observational data. Fig.1 shows the value of  $M_{BH}/M$  for, in particular, globular clusters  $M15$  and  $G1$  and highly spherical ‘elliptical’ galaxies  $M32$ ,  $M87$  and  $NGC\ 4374$ , showing that this ratio lies close to the ‘ $\alpha/2$ -line’, where  $\alpha$  is the fine structure constant  $\approx 1/137$ . However for the spiral galaxies their  $M_{DM}/M$  values do not cluster close to the  $\alpha/2$ -line. Hence it is suggested that these spherical systems manifest the minimal black hole dynamics outlined above. However this dynamics is universal, so that any spherical system must induce such a minimal black hole mode, but for which outside of such a system only the Newtonian inverse square law would be apparent. So this mode must also apply to the earth, which is certainly a surprising prediction. However just such an effect has manifested in measurements of  $g$  in mine shafts and bore holes since the 1980’s. It will now be shown that data from these geophysical measurements give us a very accurate determination of the value of  $\alpha$  in (5).

## 5 Bore Hole $g$ Anomaly

To understand this bore hole anomaly we need to compute the expression for  $g(r)$  just beneath and just above the surface of the earth. To lowest order in  $\alpha$  the ‘dark-matter’ density in (16) is substituted into (14) finally gives via (1) the acceleration

$$g(r) = \begin{cases} \frac{(1 + \frac{\alpha}{2})GM}{r^2}, & r > R, \\ \frac{4\pi G}{r^2} \int_0^r s^2 ds \rho(s) + \frac{2\pi\alpha G}{r^2} \int_0^r \left( \int_s^R s' ds' \rho(s') \right) ds, & r < R, \end{cases} \quad (18)$$

This gives Newton’s ‘inverse square law’ for  $r > R$ , but in which we see that the effective Newtonian gravitational constant is  $G_N = (1 + \frac{\alpha}{2})G$ , which is different to the fundamental gravitational constant  $G$  in (2). This caused by the additional ‘dark matter mass’ in (17). Inside the earth we see that (18) gives a  $g(r)$  different from Newtonian gravity. This has actually been observed in mine/borehole measurements of  $g(r)$  [2, 3, 4], though of course there had been no explanation for the effect, and indeed the reality of the effect was eventually doubted. The effect is that  $g$  decreases more slowly with depth than predicted by Newtonian gravity. Here the corresponding Newtonian form for  $g(r)$  is

$$g(r)_{Newton} = \begin{cases} \frac{G_N M}{r^2}, & r > R, \\ \frac{4\pi G_N}{r^2} \int_0^r s^2 ds \rho(s), & r < R, \end{cases} \quad (19)$$

with  $G_N = (1 + \frac{\alpha}{2})G$ . The gravity residual is defined as the difference between the Newtonian  $g(r)$  and the measured  $g(r)$ , which we here identify with the  $g(r)$  from (18),

$$\Delta g(r) \equiv g(r)_{Newton} - g(r)_{observed}. \quad (20)$$

Then  $\Delta g(r)$  is found to be, to 1st order in  $R - r$ , i.e. near the surface,

$$\Delta g(r) = \begin{cases} 0, & r > R, \\ -2\pi\alpha G_N \rho(R)(R - r), & r < R, \end{cases} \quad (21)$$

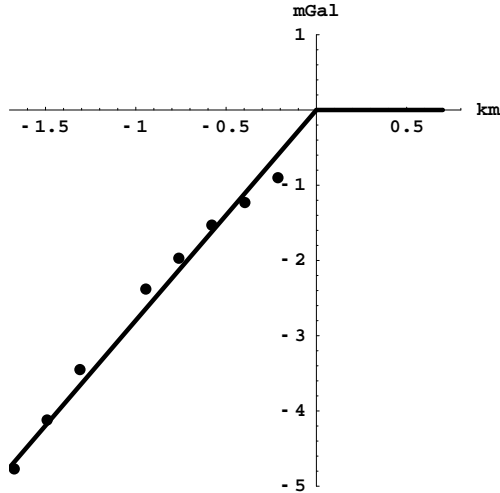


Figure 2: The data shows the gravity residuals for the Greenland Ice Cap [4] measurements of the  $g(r)$  profile, defined as  $\Delta g(r) = g_{Newton} - g_{observed}$ , and measured in mGal ( $1\text{mGal} = 10^{-3} \text{ cm/s}^2$ ), plotted against depth in km. Using (21) we obtain  $\alpha^{-1} = 139 \pm 5$  from fitting the slope of the data, as shown.

which is the form actually observed [4], as shown in Fig.2.

Gravity residuals from a bore hole into the Greenland Ice Cap were determined down to a depth of 1.5km. The ice had a measured density of  $\rho = 930 \text{ kg/m}^3$ , and from (21), using  $G_N = 6.6742 \times 10^{-11} \text{ m}^3\text{s}^{-2}\text{kg}^{-1}$ , we obtain from a linear fit to the slope of the data points in Fig.2 that  $\alpha^{-1} = 139 \pm 5$ , which equals the value of the fine structure constant  $\alpha^{-1} = 137.036$  to within the errors, and for this reason we identify the constant  $\alpha$  in (5) as being the fine structure constant. Then we arrive at the conclusion that there is indeed ‘black hole’ or ‘dark matter’ dynamics within the earth, and that from (17) we have again for the earth that  $M_{BH}/M = \alpha/2$ , as is also shown in Fig.1.

This ‘minimal black hole’ effect must also occur within stars, although that could only be confirmed by indirect observations. This effect results in  $g(r)$  becoming large at the center, unlike Newtonian gravity, which would affect nuclear reaction rates. This effect may already have manifested in the solar neutrino count problem [9, 10]. To study this will require including the new gravity dynamics into solar models.

## 6 Spiral Galaxies

We now consider the situation in which matter in-falls around an existing primordial black hole. Immediately we see some of the consequences of this time evolution: (i) because the acceleration field falls off much slower than the Newtonian inverse square law, as in (9), this in-fall would happen very rapidly, and (ii) the resultant in-flow would result in the matter rotating much more rapidly than would be predicted by Newtonian gravity, (iii) so forming a quasar which, after the in-fall of some of the matter into the black hole has ceased, would (iv) result in a spiral galaxy exhibiting non-Keplerian rotation of stars and gas clouds, *viz* the so-called ‘dark matter’ effect. The study of this time evolution will be far from simple. Here we simply illustrate the effectiveness of the new theory of gravity in explaining this ‘dark matter’ or non-Keplerian rotation-velocity effect.

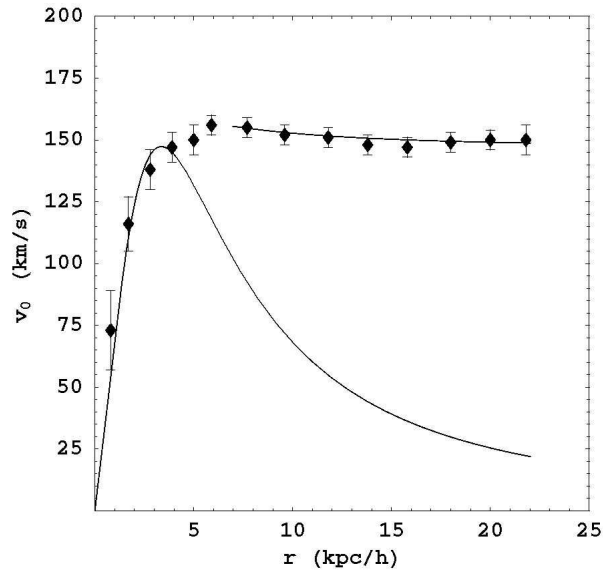


Figure 3: Data shows the non-Keplerian rotation-speed curve  $v_O$  for the spiral galaxy NGC 3198 in km/s plotted against radius in kpc/h. Lower curve is the rotation curve from the Newtonian theory for an exponential disk, which decreases asymptotically like  $1/\sqrt{r}$ . The upper curve shows the asymptotic form from (24), with the decrease determined by the small value of  $\alpha$ . This asymptotic form is caused by the primordial black holes at the centres of spiral galaxies, and which play a critical role in their formation. The spiral structure is caused by the rapid in-fall towards these primordial black holes.

We can determine the star orbital speeds for highly non-spherical galaxies in the asymptotic region by solving (15), for asymptotically where  $\rho \approx 0$  the velocity field will be approximately spherically symmetric and radial; nearer in we would match such a solution to numerically determined solutions of (5). Then (15) has an exact non-perturbative two-parameter ( $K$  and  $R_S$ ) analytic solution,

$$v(r) = K \left( \frac{1}{r} + \frac{1}{R_S} \left( \frac{R_S}{r} \right)^{\frac{\alpha}{2}} \right)^{1/2} \quad (22)$$

This velocity field then gives using (1) the non-Newtonian asymptotic acceleration

$$g(r) = \frac{K^2}{2} \left( \frac{1}{r^2} + \frac{\alpha}{2rR_S} \left( \frac{R_S}{r} \right)^{\frac{\alpha}{2}} \right), \quad (23)$$

applicable to the outer regions of spiral galaxies. We then compute circular orbital speeds using  $v_O(r) = \sqrt{rg(r)}$  giving the predicted ‘universal rotation-speed curve’

$$v_O(r) = \frac{K}{2} \left( \frac{1}{r} + \frac{\alpha}{2R_S} \left( \frac{R_S}{r} \right)^{\frac{\alpha}{2}} \right)^{1/2} \quad (24)$$

Because of the  $\alpha$  dependent part this rotation-speed curve falls off extremely slowly with  $r$ , as is indeed observed for spiral galaxies. This is illustrated in Fig.3 for the spiral galaxy NGC 3198.

## 7 Conclusion

The observational and experimental data confirm that the massive black holes in globular clusters and galaxies are necessary phenomena within a theory for gravity which uses a velocity field as the fundamental degree of freedom. This involves two constants  $G$  and  $\alpha$  and the data reveals that  $\alpha$  is the fine structure constant. This suggests that the spatial self-interaction dynamics, which is missing in the Newtonian theory of gravity, may be a manifestation at the classical level of the quantum behaviour of space. It also emerges that the ‘black hole’ effect and the ‘dark matter’ effect are one phenomenon, namely the non-Newtonian acceleration caused by singular solutions. This effect must manifest in planets and stars, and the bore hole  $g$  anomaly confirms that for planets. For stars it follows that the structure codes should be modified to include the new spatial self-interaction dynamics, and to determine the effect upon neutrino count rates. The data shows that spherical systems with masses varying over 15 orders of magnitude exhibit the  $\alpha$ -dependent dynamical effect. The non-Newtonian gravitational acceleration of primordial black holes will cause rapid formation of quasars and stars, explaining why recent observations have revealed that these formed very early in the history of the universe. In this way the new theory of gravity makes the big bang theory compatible with these recent observations. These developments clearly have major implications for cosmology and fundamental physics.

This research is supported by an Australian Research Council Discovery Grant

## References

- [1] Cahill, R.T. 2005, in *Trends in Dark Matter Research*, ed. Blain J. Val, Nova Science Pub, NY; Apeiron, **12**, No.2, 155-177.
- [2] Stacey, F.D. et al. 1981, *Phy. Rev D*, **23**, 2683.
- [3] Holding, S.C., Stacey, F.D. & Tuck, G.J. 1986, *Phys. Rev. D*, **33**, 3487.
- [4] Ander, M.E. et al. 1989, *Phys. Rev. Lett.*, **62**, 985.
- [5] Gerssen, J., van der Marel, R.P., Gebhardt, K., Guhathakurta, P., Peterson, R.C. & Pryor, C., 2002, *AJ.*, **124**, 3270; Addendum 2003, 125, 376.
- [6] Murphy, B.W., Cohn, H.N., Lugger, P.N. & Dull, J.D. 1994, *BAAS*, **26**, No.4, 1487.
- [7] Gebhardt, K., Rich, R.M. & Ho, L. C., 2002, *Astrophysics J.*, **L41**, 578.
- [8] Kormendy, J. & Richstone, D. 1995, *A & A*, **33**, 581.
- [9] Davies, R. 1964, *Phys. Rev. Lett.*, **12**, 300.
- [10] Bahcall, J. 1964, *Phys. Rev. Lett.*, **12**, 303.